RESEARCH ARTICLE

Differential modulation for asynchronous two-way relay systems over frequency-selective fading channels

Ahmad Salim[1]* and Tolga M. Duman[2]

[1] Department of Electrical and Computer Engineering, University of Illinois at Chicago, Illinois, U.S.A.
[2] Department of Electrical and Electronics Engineering (EEE), Bilkent University, Ankara 06800, Turkey

ABSTRACT

We propose two schemes for asynchronous multi-relay two-way relay (MR-TWR) systems in which neither the users nor the relays know the channel state information. In an MR-TWR system, two users exchange their messages with the help of N_R relays. Most of the existing works on MR-TWR systems based on differential modulation assume perfect symbol-level synchronization between all communicating nodes. However, this assumption is not valid in many practical systems, which makes the design of differentially modulated schemes more challenging. Therefore, we design differential modulation schemes that can tolerate timing misalignment under frequency-selective fading. We investigate the performance of the proposed schemes in terms of either probability of bit error or pairwise error probability. Through numerical examples, we show that the proposed schemes outperform existing competing solutions in the literature, especially for high signal-to-noise ratio values. Copyright © 2016 John Wiley & Sons, Ltd.

1. INTRODUCTION

Most of the existing schemes for two-way relay (TWR) systems assume known channel state information (CSI) (e.g., [1,2] and the references therein). Because of many reasons, such as the large overhead of the channel estimation process or relatively rapid variations of the channel, perfect CSI is not always available. In such scenarios, using a modulation scheme like differential phase shift keying that requires no CSI is a practical solution.

While there have been significant research efforts on using differential modulation (DM) for TWR systems, most, for example [3], assume symbol-level synchronization among all nodes. In practice, many reasons such as having different propagation delays or different dispersive channels, lead to a timing misalignment between the arriving signals. Therefore, having a perfectly synchronized TWR system is very difficult which, in return, renders the design of differentially modulated schemes more challenging. In the case of synchronous TWR systems, many schemes were proposed to address the absence of CSI, for example [3–7]. However, little work has been conducted to tackle asynchronous communication scenarios. One scenario of particular interest is the use of asynchronous multi-relay two-way relay (MR-TWR) systems in which timing errors not only occur at the end-users but at relays as well.

In [4], the authors propose a DM scheme along with maximum likelihood (ML) detection and several suboptimal solutions for a number of relaying strategies when CSI is not available at any node. The authors further extend their results to the multi-antenna case based on differential unitary space–time modulation. A simple amplify-and-forward (AF) scheme is proposed in [3] based on DM in which the self-interference term is estimated and removed prior to detection. The resulting bit error rate (BER) and the optimum power allocation strategies are also studied. In [8], the authors propose a joint relay selection and AF scheme using DM. The scheme selects the relay that minimizes the maximum BER of the two sources. Ref. [5] proposes a DM scheme that uses K parallel relays, for which a denoising function is derived to detect the sign change of the network coded symbol at each relay which is employed later by the users for detection. The paper obtains a closed form expression for the BER for the single-relay case along with a sub-optimal power allocation scheme. Furthermore, the authors derive lower and upper bounds on the BER for the multi-relay case. A low complexity

differential phase shift keying-based scheme is proposed in [6] for physical-layer network coding to acquire the network coded symbol at the relay without requiring CSI knowledge. Compared with the schemes in [4,5] which require more complexity, this scheme shows better performance at high signal-to-noise ratios (SNRs). However, the detector is only derived for a binary alphabet. In [7], the authors propose a transmission and detection scheme for a differentially-modulated, two-way satellite relaying system in which a satellite relays signals between two earth stations. The authors derive a simple suboptimum detection rule and optimize rotation angles for the two users' constellations to improve the accuracy of channel estimation.

A few proposals in the literature consider the design of distributed space–time coding (DSTC) coupled with differential modulation for synchronous TWR systems, for example, [9–11]. The models in [9,10] assume two-phase transmission and the lack of a direct link between the two users. On the other hand, [11] assumes a three-phase transmission and that a direct link between the two users exists.

All the solutions discussed above have strict synchronization requirements for proper operation. Only a few works consider asynchronous TWR systems where DM is used to mitigate absence of CSI. For instance, [12] proposes an interference cancelation scheme to reduce the interference from neighboring symbols caused by imperfect synchronization. Ref. [13] extends the scheme in [12] to dual-relay TWR systems. Similar results are reported in [14,15] for the conventional one-way relay channel. However, the schemes in [14,15] are closer to the traditional differential modulation in the sense that the self-interference term, that exist for the case of TWR systems, is absent. For TWR systems, this term consists of N_R faded (and possibly misaligned) copies of the considered user's signal, and as the fading coefficients are unknown, the schemes in [12,13] estimate this term to be able to detect the partner's message.

While [12,13] present important results, they are restricted to flat fading channels, and the delays that can be tolerated are only within the period of a symbol, which make them suitable neither for time-dispersive channels nor for systems experiencing large relative propagation delays. In this paper, we consider a more general frequency-selective fading channel model and propose two schemes that can tolerate larger relative propagation delays compared with [12]. Specifically, we first propose the joint blind-differential (JBD) detection scheme in which we first perform blind channel estimation to be able to remove the self-interference component, and then perform differential detection. We provide an approximate closed form expression for the BER for large SNR values. We then propose a scheme that is based on differential DSTC, referred to as JBD-DSTC, to fully harness the available diversity in the system. The JBD-DSTC scheme significantly reforms the JBD scheme in order to obtain an STC structure for the partner's message at each user. The pairwise error prob-ability of this scheme along with the achievable diversity is also discussed.
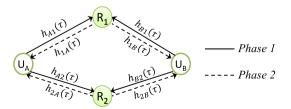
The remainder of this paper is organized as follows. Section 2 describes the system model. Section 3 details the transmission mechanism and receiver design for the proposed JBD scheme along with providing a closed form expression for the probability of error. Section 4 presents the JBD-DSTC scheme and the relevant performance analysis in terms of the pairwise error probability (PEP). Section 5 presents numerical results obtained to evaluate the performance of the proposed solutions. Finally, conclusions are drawn in Section 6.

Notation: Unless stated otherwise, bold-capital letters refer to frequency-domain vectors, bold-lower case letters refer to time-domain vectors, capital letters refer to matrices or elements of frequency-domain vectors (depending on the context), and lower-case letters refer to scalars or elements of time-domain vectors. If used as a superscript, the symbols T, $*$ and H refer to transpose, element-wise complex conjugate and Hermitian (conjugate transpose), respectively. The notation $\mathbf{0}_N$ and $0_{N \times N}$ refer to length-N all-zero column vector and $N \times N$ all-zero matrix, respectively. F is the normalized discrete Fourier transform (DFT) matrix of size-N. The Inverse DFT (IDFT) matrix of size-N is denoted by F^H. The subscript ir refers to the channel from node i to node r.

2. SYSTEM MODEL

We consider a two-phase communication scheme using AF relaying (as shown in Figure 1 for the case of two relays). The users exchange data by first simultaneously transmitting their messages to the relays during the multiple-access phase. During the broadcast phase, each relay broadcasts an amplified version of its received signal which is a noisy summation of the users' messages.

Each user transmits M blocks that comprise one frame. Prior to transmission, each block is modulated using orthogonal frequency division multiplexing (OFDM) with N subcarriers. Each one of the resulting blocks is appended with a cyclic-prefix (CP). We model asynchrony by assuming different propagation delays. For proper CP design, user U_i, $i \in \{A, B\}$, requires the knowledge of the worst-case scenario propagation delays over the links connecting it to the relays, that is, d_{ir} (in multiples of the sampling time), $r \in \{1, 2, \ldots, N_R\}$. Similarly, the rth relay, $r \in \{1, 2, \ldots, N_R\}$, requires d_{ri}, $i \in \{A, B\}$.

Figure 1. The multi-relay two-way relay system model (for $N_R = 2$).

The multipath fading channels from the users to the relays are modeled (in the equivalent low-pass signal domain) by the discrete channel impulse responses (CIRs) $h_{ir,l}$, $i \in \{A, B\}$, $r \in \{1, 2, \ldots, N_R\}$, $l \in \{1, 2, \ldots, L_{ir}\}$, where L_{ir} represents the number of resolvable paths. Similarly, the channels from the relays to the users are modeled by $h_{ri,l}$. The overall channel response over the L_{ir} lags can be expressed as $h_{ir}(\tau) = \sum_{l=1}^{L_{ir}} h_{ir,l}\delta\left(\tau - \tau_{ir,l}\right)$, where τ is the lag index and $\tau_{ir,l}$ is the delay of the lth path normalized by the sampling period T_S. We assume quasi-static frequency-selective fading in which $h_{ir,l}$ remain constant for all the blocks over the same lag (l) and change independently across the different lags. We assume that $h_{ir,l}$ is a circularly-symmetric complex Gaussian (CSCG) random variable (RV) with zero mean and variance of $\sigma_{ir,l}^2$. Also, the channel coefficients are independent across different links. We assume half-duplex operation at all nodes.

For the JBD scheme, we further assume that the channels on the same link are reciprocal, that is, $h_{ir}(\tau) = h_{ri}(\tau)$ $\forall i, r$. Also, the uplink and downlink propagation delays over the same link are assumed to be identical.

3. THE JOINT BLIND-DIFFERENTIAL SCHEME

In this scheme, each user uses N parallel differential encoders; each operating on a specific subcarrier. The data vector representing the frequency-domain message of the ith user, $i \in \{A, B\}$, during the mth block is denoted by $X_i^{(m)}$ where $X_i^{(m)} = \left[X_{i,1}^{(m)}, X_{i,2}^{(m)}, \ldots, X_{i,N}^{(m)}\right]^T$ and $X_{i,k}^{(m)} \in \mathcal{A}_i$ where $\mathcal{A}_i$ is a unit-energy, zero-mean, phase-shift keying (PSK) constellation set that is closed under multiplication, for example, the set $\{\pm 1, \pm j\}$, to maintain the transmit power at a specific level. We remark that the encoders (and decoders) in this paper are designed for the earlier assumptions. However, they can be modified to account for constellations that do not follow these assumptions such as quadrature amplitude modulation. In this case, encoding and decoding can be performed using a look-up table approach instead of a rule (as in [16]).

Using DM, the differentially encoded symbol over the kth subcarrier of the mth block can be expressed as $S_{i,k}^{(m)} = X_{i,k}^{(m)} S_{i,k}^{(m-1)}$, $m \in \{2, 3, \ldots, M\}$, and $S_{i,k}^{(1)} = X_{i,k}^{(1)}$. After performing IDFT, we obtain $s_i^{(m)} = \left[s_{i,1}^{(m)}, s_{i,2}^{(m)}, \ldots, s_{i,N}^{(m)}\right]^T = \text{IDFT}(S_i^{(m)})$. The transmitted signal from the ith user during the mth block, $i \in \{A, B\}$, is given by:

$$s_{Tx,i}^{(m)} = \sqrt{P_i}\zeta_1\left(s_i^{(m)}\right) \qquad (1)$$

where $s_{Tx,i}^{(m)} = \left[s_{Tx,i,1}^{(m)}, s_{Tx,i,2}^{(m)}, \ldots, s_{Tx,i,N+N_{CP,1}}^{(m)}\right]^T$, P_i, $i \in \{A, B\}$, is the transmission power at the ith user and $\zeta_1(\cdot)$ corresponds to the operation of appending a length $N_{CP,1}$ CP to the vector in its argument at each user prior to the

first phase of transmission. The length of this CP is selected to satisfy $N_{CP,1} \geq \max_{i,r}\{L_{ir} + d_{ir}\}$, $i \in \{A, B\}$, $r \in \{1, 2\}$.

3.1. Relay processing

Having appended a CP of the proper length at each user, the received signal corresponding to the mth block at the rth relay after removing the CP is given by

$$y_r^{(m)} = \sqrt{P_A}H_{tl,Ar}\Psi_{d_{Ar}}s_A^{(m)} + \sqrt{P_B}H_{tl,Br}\Psi_{d_{Br}}s_B^{(m)} + n_r^{(m)},$$

where $H_{tl,ir}$ is the time-lag channel matrix corresponding to the channel over the link ir, and $n_r^{(m)}$ represents length-N noise vector at the rth relay during the mth block whose entries are independent and identically distributed CSCG RVs with zero mean and variance of σ_r^2. $\Psi_{d_{ir}}$, $i \in \{A, B\}$, $r \in \{1, 2, \ldots, N_R\}$, is a circulant matrix of size $N \times N$ whose first column is given by the $N \times 1$ vector $\psi_{d_{ir}} = \left[\mathbf{0}_{d_{ir}}^T, 1, \mathbf{0}_{N-d_{ir}-1}^T\right]^T$. Using the matrix $\Psi_{d_{ir}}$ mimics the circular shift caused by having a propagation delay of d_{ir} samples. To simplify blind channel estimation at the end user, R_r performs conjugation and time-reversal operations to obtain $s_r^{(m)} = \eta\left(y_r^{(m)*}\right)$ where $\eta(\cdot)$ is the time-reversal operator. For $x = [x_1, x_2, \ldots, x_N]^T$, $\eta(\cdot)$ is defined element-wise as $\eta(x_n) \triangleq x_{N-n+2}$, $n = 1, \ldots, N$ and $x_{N+1} \triangleq x_1$. The conjugation and reversal in the time-domain will have a conjugation effect in the frequency-domain after taking DFT at the end user.

After processing the mixture of signals, R_r appends a CP for the second phase of transmission of length $N_{CP,2}$ that satisfies $N_{CP,2} \geq \max_{r,i}\{L_{ri} + d_{ri}\}$, $r \in \{1, 2, \ldots, N_R\}$, $i \in \{A, B\}$. The rth relay transmitted signal is given by

$$s_{Tx,r}^{(m)} = \sqrt{P_r G_r}\zeta_2\left(s_r^{(m)}\right), \quad r \in \{1, 2\} \qquad (2)$$

where $s_{Tx,r}^{(m)} = \left[s_{Tx,r,1}^{(m)}, s_{Tx,r,2}^{(m)}, \ldots, s_{Tx,r,N+N_{CP,2}}^{(m)}\right]^T$, P_r and G_r are the transmission power and the scaling factor at the rth relay, respectively, and $\zeta_2(\cdot)$ corresponds to the operation of appending a length $N_{CP,2}$ CP to the vector in its argument.

3.2. Detection at the end-user

Because of symmetry, we only describe detection at user B. After removing the CP that was added at the relays, the received N-sample OFDM blocks can be written as

$$y_B^{(m)} = \sum_{r=1}^{N_R} \sqrt{P_A P_r G_r}H_{tl,rB}\Psi_{d_{rB}}\eta\left(H_{tl,Ar}^*\Psi_{d_{Ar}}^*s_A^{(m)*}\right)$$
$$+ \sum_{r=1}^{N_R} \sqrt{P_B P_r G_r}H_{tl,rB}\Psi_{d_{rB}}\eta\left(H_{tl,Br}^*\Psi_{d_{Br}}^*s_B^{(m)*}\right)$$
$$+ v_B^{(m)},$$

where $v_B^{(m)}$ represents length-N effective noise vector at user B during the mth block which encompasses the relays' amplified noise as well. The entries of $v_B^{(m)}$ are independent and identically distributed CSCG RVs with zero mean and variance of $\sigma_{B,eff}^2 = \sigma_B^2 + \sum_{r=1}^{N_R} G_r P_r \left|[H_{df,rB}]_{k,k}\right|^2 \sigma_r^2$ where σ_B^2 is the variance of the original noise terms at user B.

Let $V_B^{(m)} = F v_B^{(m)}$, $P_{ir} = P_i P_r G_r$ and assume that $d_{ri} = d_{ir}$, $r \in \{1, 2, \ldots, N_R\}$, $i \in \{A, B\}$. After performing DFT and noting that $F\eta(x^*) = (Fx)^*$, the received signal on the kth subcarrier of the mth block simplifies to† $Y_{B,k}^{(m)} = \mu_k S_{B,k}^{(m)*} + v_k S_{A,k}^{(m)*} + V_{B,k}^{(m)}$ where

$$v_k = \sum_{r=1}^{N_R} \sqrt{P_{Ar}} [H_{df,rB}]_{k,k} \left[H_{df,Ar}^*\right]_{k,k} e^{-j\frac{2\pi(k-1)(d_{rB}-d_{Ar})}{N}},$$

$\mu_k = \sum_{r=1}^{N_R} \sqrt{P_{Br}} \left|[H_{df,Br}]_{k,k}\right|^2$, $V_{B,k}^{(m)}$ is the kth element of $V_B^{(m)}$, and $H_{df,ir} = F H_{tl,ir} F^H$ denotes the Doppler-frequency channel matrix (also called the subcarrier coupling matrix) over the link ir which is a diagonal matrix in our case of quasi-static fading.

The results of [3] are adopted to estimate the parameter μ_k in order to remove the self-interference term. Defining, $\widetilde{Y}_{B,k}^{(m)} = X_{B,k}^{(m)*} Y_{B,k}^{(m-1)} - Y_{B,k}^{(m)}$, we can write

$$\widetilde{Y}_{B,k}^{(m)} = v_k S_{A,k}^{(m-1)*}\left(X_{B,k}^{(m)*} - X_{A,k}^{(m)*}\right) + \widetilde{V}_{B,k}^{(m)}, \quad (3)$$
$$m = 2, \ldots, M,$$

where $\widetilde{V}_{B,k}^{(m)} = X_{B,k}^{(m)*} V_{B,k}^{(m-1)} - V_{B,k}^{(m)}$. At high SNR, we can approximate $\widetilde{Y}_{B,k}^{(m)*} \widetilde{Y}_{B,k}^{(m)}$ as

$$\widetilde{Y}_{B,k}^{(m)*} \widetilde{Y}_{B,k}^{(m)} \approx |v_k|^2 \left|S_{A,k}^{(m-1)}\right|^2 \left|X_{B,k}^{(m)} - X_{A,k}^{(m)}\right|^2, \quad (4)$$
$$m = 2, \ldots, M.$$

Taking the expected value of (4) over the constellation points of $S_{A,k}^{(m-1)}$, $X_{A,k}^{(m)}$ and $X_{B,k}^{(m)}$, we note that for the RHS, it is the same for all m and k as the constellation sets $\mathcal{A}_i$, $i \in \{A, B\}$ are the same for all blocks and subcarriers. We also note that $S_{A,k}^{(m-1)}$ is independent from both $X_{B,k}^{(m)}$ and $X_{A,k}^{(m)}$. For a sufficiently large M, we can approximate the ensemble average of $\widetilde{Y}_{B,k}^{(m)*} \widetilde{Y}_{B,k}^{(m)}$ by its time average. Therefore, we can obtain an estimate of $|v_k|$, denoted by $|\widehat{v}_k|$, as

$$|\widehat{v}_k|^2 \approx \frac{\sum_{m=2}^{M} \left|\widetilde{Y}_{B,k}^{(m)}\right|^2}{(M-1)\mathbb{E}\left[\left|S_{A,k}^{(m-1)}\right|^2\right] \mathbb{E}\left[\left|X_{B,k}^{(m)} - X_{A,k}^{(m)}\right|^2\right]}, \quad (5)$$

where $\mathbb{E}\left[\left|S_{A,k}^{(m-1)}\right|^2\right] = 1$ and $\mathbb{E}\left[\left|X_{B,k}^{(m)} - X_{A,k}^{(m)}\right|^2\right]$ can be calculated easily as the corresponding set defined by $\mathcal{K} = \{|b-a|^2 \mid b \in \mathcal{A}_B, a \in \mathcal{A}_A\}$ is finite. For instance, if $\mathcal{A}_i = \{1, -1\}$, $i \in \{A, B\}$, then $\mathcal{K} = \{0, 4\}$ and $\mathbb{E}\left[\left|X_{B,k}^{(m)} - X_{A,k}^{(m)}\right|^2\right] = 2$. Let $Y_{B,k} = \left[Y_{B,k}^{(1)}, Y_{B,k}^{(2)}, \ldots, Y_{B,k}^{(M)}\right]^T$. If M is sufficiently large, we can approximate $Y_{B,k}^H Y_{B,k}$ as

$$Y_{B,k}^H Y_{B,k} \approx M\left(\mu_k^2 + |v_k|^2 + \sigma_{V_B}^2\right). \quad (6)$$

At high SNR, we can write

$$\mu_k^2 + |v_k|^2 \approx \frac{Y_{B,k}^H Y_{B,k}}{M}. \quad (7)$$

Therefore, we can estimate μ_k as

$$\widehat{\mu}_k \approx \sqrt{\left(\frac{Y_{B,k}^H Y_{B,k}}{M} - |\widehat{v}_k|^2\right) \mathrm{U}\left(\frac{Y_{B,k}^H Y_{B,k}}{M} - |\widehat{v}_k|^2\right)}, \quad (8)$$

where $\mathrm{U}(.)$ is the Heaviside unit step function. Now, we can remove the estimated self-interference term, namely $\widehat{\mu}_k S_{B,k}^{(m)*}$ to obtain

$$\begin{aligned} Y_{AB,k}^{(m)} &\triangleq Y_{B,k}^{(m)} - \widehat{\mu}_k S_{B,k}^{(m)*} \\ &\approx v_k S_{A,k}^{(m)*} + V_{B,k}^{(m)}, \quad m = 1, \ldots, M. \end{aligned} \quad (9)$$

We can further express $Y_{AB,k}^{(m)}$ as

$$Y_{AB,k}^{(m)} \approx X_{A,k}^{(m)*} Y_{AB,k}^{(m-1)} + \left(V_{B,k}^{(m)} - X_{A,k}^{(m)*} V_{B,k}^{(m-1)}\right), \quad (10)$$
$$m = 2, \ldots, M.$$

Therefore, we write the following symbol-by-symbol ML detection rule to recover $X_{A,k}^{(m)}$ at user B

$$\widehat{X}_{A,k}^{(m)} = \arg\min_{X \in \mathcal{A}_A} \left|Y_{AB,k}^{(m)} - X^* Y_{AB,k}^{(m-1)}\right|^2 \quad (11)$$

$$= \arg\max_{X \in \mathcal{A}_A} \mathrm{Re}\left\{Y_{AB,k}^{(m)} Y_{AB,k}^{(m-1)*} X\right\}, \quad m = 2, \ldots, M. \quad (12)$$

We remark that better performance can be attained if multiple-symbol differential detection, as in [17], is used. However, the detection complexity will be greater.

---

†Refer to Appendix A for details.

3.3. Performance analysis

In this section, we provide an approximate closed form expression for the probability of error of the JBD scheme by using results from the frequency-flat, Rayleigh-faded, single-way relay systems in [3,18].

Assume that instead of using G_r to normalize the power at the rth relay in time domain, we use $G_{r,k}$ to normalize the power of the kth subcarrier in frequency domain. Note that $G_{r,k}$ can be estimated for large M as $G_{r,k} \approx \frac{M}{||Y_{r,k}||^2}$ without any CSI knowledge at the relay where $Y_{r,k} = \left[Y_{r,k}^{(1)}, Y_{r,k}^{(2)}, \ldots, Y_{r,k}^{(M)} \right]$ and $Y_r^{(m)} = \left[Y_{r,1}^{(m)}, Y_{r,2}^{(m)}, \ldots, Y_{r,N}^{(m)} \right]^T = \text{DFT}\left(y_r^{(m)} \right)$. By modeling the JBD system by an equivalent coherent receiver with treating v_k as a known channel gain and $\left(V_{B,k}^{(m)} - X_{A,k}^{(m)*} V_{B,k}^{(m-1)} \right)$ as the equivalent noise term, we can approximate the effective SNR over the kth subcarrier at user B as

$$\gamma_{B,k} \approx \frac{|v_k|^2}{2\text{Var}\left[V_{B,k}^{(m)} \right]} \tag{13}$$

$$= \frac{P_A \sum_{r=1}^{N_R} P_r |q_{rB,k}|^2 |q_{Ar,k}|^2 + P_A \sum_{i=1}^{N_R} \sum_{j=1,j\neq i}^{N_R} \sqrt{P_i P_j G_{i,k} G_{j,k}} q_{iB,k} q_{Ai,k}^* q_{jB,k}^* q_{Aj,k}}{2\left(\sigma_B^2 + \sum_{r=1}^{N_R} G_{r,k} P_r |q_{rB,k}|^2 \sigma_r^2 \right)}, \tag{14}$$

where $q_{ij,k} = \left[H_{df,ij} \right]_{k,k}$ and $\text{Var}[\cdot]$ is the variance operator.

As $\gamma_{B,k}$ in (13) is a complicated function of $2N_R$ Rayleigh-distributed RVs, finding its statistics (PDF, CDF, etc.) is difficult, and hence deriving the probability of error is intractable. However, an important result in [18] for a special choice of the scaling factor simplifies the analysis as it results in expressing the effective SNR in terms of the harmonic mean of the instantaneous SNR of the two hops, which in turn simplifies the calculations. The adopted scaling factor normalizes the power of the kth subcarrier as $G_{r,k} = \left(P_A \left| \left[H_{df,Ar} \right]_{k,k} \right|^2 + P_B \left| \left[H_{df,Br} \right]_{k,k} \right|^2 + \sigma_r^2 \right)^{-1}$. At this point, we adopt this scaling factor to make the analysis tractable for the JBD scheme.

Assume that $\sigma_i^2 = \sigma_r^2 = \sigma^2 \ \forall \ i \in \{A, B\}$, $r \in \{1, 2, \ldots, N_R\}$ and let $\gamma_1 = \frac{P_A}{\sigma^2}$ and $\gamma_2 = \frac{\sum_{r=1}^{N_R} P_r}{\sigma^2}$ be the per-hop SNRs for the first and second hops, respectively. Assuming that the CIRs are normalized such that $\sum_{l=1}^{L_{ir}} \sigma_{ir,l}^2 = 1$, $i \in \{A, B\}$, $r \in \{1, 2, \ldots, N_R\}$, we have $|q_{ir,k}| \sim Rayleigh\left(\frac{1}{\sqrt{2}} \right)$ and $|q_{ri,k}| \sim Rayleigh\left(\frac{1}{\sqrt{2}} \right)$. By dropping the second term of the numerator of (14) and using γ_2 as the SNR for the second hop, the performance of the JBD scheme can be approximated by the performance of the single relay systems in [3,18].

Assuming Binary PSK (BPSK) modulation, the average probability of bit error at user B in the high SNR region can be approximated in terms of the per-relay SNR (i.e., γ_1) and the SNR of the second hop linking the relays to user B (i.e., γ_2) as

$$P_{e,B} \approx \frac{1}{\gamma_1} + \frac{1}{2\gamma_2}. \tag{15}$$

We finally note that dropping the cross terms in the numerator of (14) has the advantage of mathematical tractability, and as the numerical examples will show later on, the approximation closely match the actual system performance, especially for high SNR values.

4. THE DISTRIBUTED SPACE–TIME CODING-BASED JOINT BLIND-DIFFERENTIAL SCHEME

In multi-antenna single-way relay systems, DSTC was proposed in [19] based on linear dispersion space-time codes (STCs) to mimic having an STC structure at the destination similar to the one obtained in multi-input single-output systems that uses STCs. The system in [19] assumes that there is CSI knowledge only at the destination. When there is no CSI knowledge, the differential DSTC can be used [20].

In this section, we describe the proposed JBD-DSTC scheme based on differential DSTC transmission for a multi-relay TWR system in order to fully harness the inherent diversity advantage of this system. We consider a frame composed of M blocks in which T blocks are grouped together. There are M_G groups in a frame where $M_G = M/T$, and the symbols over one subcarrier from the blocks of each group correspond to one space–time codeword.

Figure 2 illustrates the encoding process at the ith user for the T symbols over the kth subcarrier during the mth group. Note that N parallel encoders are required for the entire N subcarriers. As shown in Figure 2, the frequency-domain data-bearing vector of the ith user, $i \in \{A, B\}$, during the tth block of the mth group is denoted by $X_i^{(m,t)}$ where $X_i^{(m,t)} = \left[X_{i,1}^{(m,t)}, X_{i,2}^{(m,t)}, \ldots, X_{i,N}^{(m,t)} \right]^T$ and $X_{i,k}^{(m,t)} \in \mathcal{A}_i$. Prior to differential encoding, the vector of data symbols over the same subcarrier, k, and over all blocks of the same group, m, that is, $X_{i,k}^{(m)} = \left[X_{i,k}^{(m,1)}, X_{i,k}^{(m,2)}, \ldots, X_{i,k}^{(m,T)} \right]^T$, is encoded as a $T \times T$ unitary
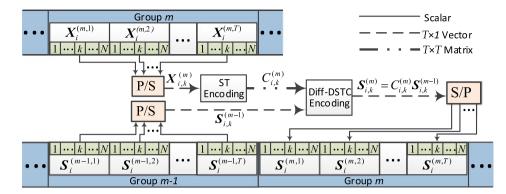
Figure 2. Encoding process of the joint blind-differential-distributed space–time coding (DSTC) scheme at the ith user for the T symbols over the kth subcarrier during the mth group. The green boxes represent the symbols on the N subcarriers for the corresponding block and the notations P/S and S/P denote parallel to serial and serial to parallel, respectively. ST, space–time.

matrix $C_{i,k}^{(m)}$. The structure of this matrix is designed such that it commutes with the linear dispersion matrices at the relays [20]. Let $\mathcal{C}$ denote the set of all possibilities of such matrices. Note that having a unitary structure preserves the transmit power at each user.

Using differential DSTC, each user differentially encodes the T symbols on the kth subcarrier of the T blocks belonging to the mth group as $S_{i,k}^{(m)} = C_{i,k}^{(m)} S_{i,k}^{(m-1)}$, $m \in \{2,3,\ldots,M_G\}$ where $S_{i,k}^{(m)} = \left[S_{i,k}^{(m,1)}, S_{i,k}^{(m,2)}, \ldots, S_{i,k}^{(m,T)} \right]^T$ and $S_{i,k}^{(1)}$ is an arbitrary $T \times 1$ reference vector with elements from $\mathcal{A}_i$. Let $S_i^{(m,t)} = \left[S_{i,1}^{(m,t)}, S_{i,2}^{(m,t)}, \ldots, S_{i,N}^{(m,t)} \right]^T$. After performing IDFT, we obtain $s_i^{(m,t)} = \left[s_{i,1}^{(m,t)}, s_{i,2}^{(m,t)}, \ldots, s_{i,N}^{(m,t)} \right]^T = \mathrm{IDFT}\left(S_{ix}^{(m,t)} \right)$. The transmitted signal from the ith user during the tth block of the mth group, $i \in \{A,B\}$, is given by $s_{Tx,i}^{(m,t)} = s_{Tx,i}^{(m,t)} = \left[s_{Tx,i,1}^{(m,t)}, s_{Tx,i,2}^{(m,t)}, \ldots, s_{Tx,i,N+N_{CP,1}}^{(m,t)} \right]^T = \sqrt{P_i} \zeta_1 \left(s_i^{(m,t)} \right)$.

4.1. Relay processing

After CP removal during the multiple-access phase at the rth relay, the received superimposed signal for the tth OFDM block of the mth group is given by

$$y_r^{(m,t)} = \sqrt{P_A} H_{tl,Ar} \Psi_{d_{A_r}} s_A^{(m,t)} + \sqrt{P_B} H_{tl,Br} \Psi_{d_{B_r}} s_B^{(m,t)} + n_r^{(m,t)},$$

where $y_r^{(m,t)} = \left[y_{r,1}^{(m,t)}, y_{r,2}^{(m,t)}, \ldots, y_{r,N}^{(m,t)} \right]^T$ and $n_r^{(m,t)}$ is a CSCG random vector with mean $\mathbf{0}_N$ and covariance matrix $\sigma_r^2 I_N$. To obtain the desired STC structure at the end-users, the rth relay processes $\left\{ y_{r,n}^{(m,t)} \right\}_{t \in \{1,2,\ldots,T\}}$ to obtain $s_{r,n}^{(m)}$ as

$$\begin{bmatrix} s_{r,n}^{(m,1)} \\ s_{r,n}^{(m,2)} \\ s_{r,n}^{(m,3)} \\ \vdots \\ s_{r,n}^{(m,T)} \end{bmatrix} = A_r \begin{bmatrix} y_{r,n}^{(m,1)} \\ y_{r,n}^{(m,2)} \\ y_{r,n}^{(m,3)} \\ \vdots \\ y_{r,n}^{(m,T)} \end{bmatrix} + B_r \begin{bmatrix} \eta\left(y_{r,n}^{(m,1)*} \right) \\ \eta\left(y_{r,n}^{(m,2)*} \right) \\ \vdots \\ \eta\left(y_{r,n}^{(m,T)*} \right) \end{bmatrix},$$

$r = \{1,\ldots,N_R\}$, $n = \{1,\ldots,N\}$. The $T \times T$ relay dispersion matrices A_r and B_r are designed such that they commute with the data matrices, that is, with $C_{i,k}^{(m)}$, while ensuring that the received signal at each user possesses the desired space-time block code structure.

One simple design is introduced in [20] in which the relays are classified into two groups, $\mathcal{G}_1$ and $\mathcal{G}_2$. The rth relay falling into $\mathcal{G}_1$ uses a unitary matrix for A_r and sets $B_r = 0_{T \times T}$ while that falling into $\mathcal{G}_2$ sets $A_r = 0_{T \times T}$ and uses a unitary matrix for B_r. According to this design, the relays' commutative property can be written as $CO_r = O_r \widetilde{C}_r \; \forall r$ where

$$O_r = \begin{cases} A_r, & r \in \mathcal{G}_1, \\ B_r, & r \in \mathcal{G}_2, \end{cases} \quad \text{and} \quad \widetilde{C}_r = \begin{cases} C, & r \in \mathcal{G}_1, \\ C^*, & r \in \mathcal{G}_2. \end{cases}$$

Hence, we can write the set of all possible STC data matrices as

$$\mathcal{C} = \left\{ C \, \middle| \, C^H C = C C^H = I_{T \times T}, C O_r = O_r \widetilde{C}_r \forall r \right\}.$$

To simplify the estimation of the self-interference term, we impose another design criterion on the relay dispersion matrices, that is, all the matrices of the form $O_i^H O_j$, $i,j \in \{1,2,\ldots,N_R\}$, $i \neq j$, are hollow matrices, that is, their diagonal entries are all zeros.

The tth transmitted block of the rth relay during the mth group is given by $s_{Tx,r}^{(m,t)} = \sqrt{P_r G_r} \zeta_2 \left(s_r^{(m,t)} \right)$ where

$$s_{Tx,r}^{(m)} = \left[s_{Tx,r,1}^{(m)}, s_{Tx,r,2}^{(m)}, \ldots, s_{Tx,r,N+N_{CP,2}}^{(m)} \right]^T \quad \text{and}$$

$$s_r^{(m,t)} = \left[s_{r,1}^{(m,t)}, s_{r,2}^{(m,t)}, \ldots, s_{r,N}^{(m,t)} \right]^T.$$

4.2. Detection at the end-user

By the end of the braodcast phase, and after removing the CP of length $N_{CP,2}$ at user B, the resulting consecutive N-sample OFDM blocks of the tth block, $t \in \{1, 2, \ldots, T\}$, in the mth group, $m \in \{1, M_G\}$, is denoted by $\boldsymbol{y}_B^{(m,t)}$. After performing DFT, the frequency-domain signal corresponding to $\boldsymbol{y}_B^{(m,t)}$ is $\boldsymbol{Y}_B^{(m,t)} = \left[Y_{B,1}^{(m,t)}, Y_{B,2}^{(m,t)}, \ldots, Y_{B,N}^{(m,t)} \right]^T$ where $\boldsymbol{Y}_B^{(m,t)} = \mathrm{DFT}\left(\boldsymbol{y}_B^{(m,t)} \right)$. Let $\boldsymbol{V}_B^{(m,t)} = \left[V_{B,1}^{(m,t)}, V_{B,2}^{(m,t)}, \ldots, V_{B,N}^{(m,t)} \right]^T$ denote the frequency-domain noise vector observed at user B during the tth block of the mth group and let $\boldsymbol{Y}_{B,k}^{(m)} = \left[Y_{B,k}^{(m,1)}, Y_{B,k}^{(m,2)}, \ldots, Y_{B,k}^{(m,T)} \right]^T$ denote the vector of received signals from all blocks of the mth group on the kth subcarrier. Similarly, define $\boldsymbol{V}_{B,k}^{(m)} = \left[V_{B,k}^{(m,1)}, V_{B,k}^{(m,2)}, \ldots, V_{B,k}^{(m,T)} \right]^T$ and $\boldsymbol{D}_{i,k}^{(m)} = \left[O_1 \widetilde{\boldsymbol{S}}_{i,k,1}^{(m)}, O_2 \widetilde{\boldsymbol{S}}_{i,k,2}^{(m)}, \ldots, O_{N_R} \widetilde{\boldsymbol{S}}_{i,k,N_R}^{(m)} \right], i \in \{A, B\}$ where

$$\widetilde{\boldsymbol{S}}_{i,k,r}^{(m)} = \left[\widetilde{S}_{i,k,r}^{(m,1)}, \widetilde{S}_{i,k,r}^{(m,2)}, \ldots, \widetilde{S}_{i,k,r}^{(m,T)} \right]^T = \begin{cases} \boldsymbol{S}_{i,k}^{(m)}, & r \in \mathcal{G}_1, \\ \boldsymbol{S}_{i,k}^{(m)*}, & r \in \mathcal{G}_2. \end{cases}$$

Let $q_{ij,k} = \left[H_{df,ij} \right]_{k,k}$. We can write $\boldsymbol{Y}_{B,k}^{(m)}$ as[‡] $\boldsymbol{Y}_{B,k}^{(m)} = \boldsymbol{D}_{B,k}^{(m)} \boldsymbol{\mu}_{B,k} + \boldsymbol{D}_{A,k}^{(m)} \boldsymbol{\mu}_{A,k} + \boldsymbol{V}_{B,k}^{(m)}$ where $\boldsymbol{\mu}_{i,k}$, $i \in \{A, B\}$, are $N_R \times 1$ channel-dependent vectors defined as

$$\boldsymbol{\mu}_{i,k} = \begin{bmatrix} \sqrt{P_{i1}} q_{1B,k} \widetilde{q}_{i1,k} e^{-j \frac{2\pi(k-1)\left(d_{1B} + \widetilde{d}_{i1} \right)}{N}} \\ \sqrt{P_{i2}} q_{2B,k} \widetilde{q}_{i2,k} e^{-j \frac{2\pi(k-1)\left(d_{2B} + \widetilde{d}_{i2} \right)}{N}} \\ \vdots \\ \sqrt{P_{iN_R}} q_{N_R B,k} \widetilde{q}_{iN_R,k} e^{-j \frac{2\pi(k-1)\left(d_{N_R B} + \widetilde{d}_{iN_R} \right)}{N}} \end{bmatrix},$$

$$(16)$$

where

$$\widetilde{q}_{ij,k} = \begin{cases} q_{ij,k}, & j \in \mathcal{G}_1, \\ q_{ij,k}^*, & j \in \mathcal{G}_2, \end{cases} \text{ and } \widetilde{d}_{ij} = \begin{cases} d_{ij}, & j \in \mathcal{G}_1, \\ -d_{ij}, & j \in \mathcal{G}_2. \end{cases}$$

For a sufficiently large M, we can obtain an estimate of $\boldsymbol{\mu}_{B,k}$, denoted by $\widehat{\boldsymbol{\mu}}_{B,k}$, as[§]

$$\widehat{\boldsymbol{\mu}}_{B,k} \approx \sum_{m=1}^{M} \boldsymbol{D}_{B,k}^{(m)H} \boldsymbol{Y}_{B,k}^{(m)} / (MT), \qquad (17)$$

Note that unlike the JBD scheme, the JBD-DSTC scheme does not require the channel reciprocity assumption. Having obtained an estimate for $\boldsymbol{\mu}_{B,k}$, user B can remove its estimated self-interference term, $\boldsymbol{D}_{B,k}^{(m)} \widehat{\boldsymbol{\mu}}_{B,k}$ to

___

[‡]An illustrative example for a dual-relay system is given in Appendix B.

[§]The derivation of this result is outlined in Appendix C.

obtain $\boldsymbol{Y}_{AB,k}^{(m)} \approx \boldsymbol{D}_{A,k}^{(m)} \boldsymbol{\mu}_{A,k} + \boldsymbol{V}_{B,k}^{(m)}$. Using the commutative property and the fact that $\boldsymbol{S}_{i,k}^{(m)}$ is differentially encoded, we can simplify $\boldsymbol{Y}_{AB,k}^{(m)}$ as

$$\begin{aligned} \boldsymbol{Y}_{AB,k}^{(m)} &\approx \left[O_1 \widetilde{C}_{A,k,1}^{(m)} \widetilde{\boldsymbol{S}}_{A,k,1}^{(m)}, O_2 \widetilde{C}_{A,k,2}^{(m)} \widetilde{\boldsymbol{S}}_{A,k,2}^{(m)}, \right. \\ &\quad \left. \ldots, O_{N_R} \widetilde{C}_{A,k,N_R}^{(m)} \widetilde{\boldsymbol{S}}_{A,k,N_R}^{(m)} \right] \widehat{\boldsymbol{v}}_k + \boldsymbol{V}_{B,k}^{(m)} \\ &\approx \left[C_{A,k}^{(m)} O_1 \widetilde{\boldsymbol{S}}_{A,k,1}^{(m-1)}, C_{A,k}^{(m)} O_2 \widetilde{\boldsymbol{S}}_{A,k,2}^{(m-1)}, \right. \\ &\quad \left. \ldots, C_{A,k}^{(m)} O_{N_R} \widetilde{\boldsymbol{S}}_{A,k,N_R}^{(m-1)} \right] \widehat{\boldsymbol{v}}_k + \boldsymbol{V}_{B,k}^{(m)} \\ &\approx C_{A,k}^{(m)} \boldsymbol{Y}_{AB,k}^{(m-1)} + \left(\boldsymbol{V}_{B,k}^{(m)} - C_{A,k}^{(m)} \boldsymbol{V}_{B,k}^{(m-1)} \right), \\ &\quad m = 2, 3, \ldots, M_G \end{aligned} \qquad (18)$$

where

$$\widetilde{C}_{A,k,r}^{(m)} = \begin{cases} C_{A,k}^{(m)}, & r \in \mathcal{G}_1, \\ C_{A,k}^{(m)*}, & r \in \mathcal{G}_2, \end{cases}$$

Therefore, $C_{A,k}^{(m)}$ can be recovered at user B using the following detection rule

$$\widehat{C}_{A,k}^{(m)} = \arg \min_{C \in \mathcal{C}} \left\| \boldsymbol{Y}_{AB,k}^{(m)} - C \boldsymbol{Y}_{AB,k}^{(m-1)} \right\|^2, \quad m = 2, 3, \ldots, M_G. \qquad (19)$$

Note that if C has a space-time block code structure, then the above equation can be easily decoupled, which allows fast symbol-wise ML detection. Similar to the JBD scheme, employing ideas based on multiple-symbol differential detection, which in this case involves the joint detection of the M_G data matrices, promises significant performance improvements, however, it comes at the expense of increased receiver complexity.

4.3. Performance analysis

Inspired by the results obtained in [20] for single-way differential DSTC, we can write the pairwise error probability of mistaking $C_{A,k}^{(m)}$ by $C_{A,k}^{\prime(m)}$, that is, $\mathbb{P}\left(C_{A,k}^{(m)} \to C_{A,k}^{\prime(m)} \right)$ in the two-way relaying scheme under consideration. Let $\sigma_i^2 = \sigma_r^2 = \sigma^2 \; \forall \; i \in \{A, B\}, r \in \{1, 2, \ldots, N_R\}$. Assuming that the CIRs are normalized such that $\sum_{l=1}^{L_{ir}} \sigma_{ir,l}^2 = 1$, $i \in \{A, B\}, r \in \{1, 2, \ldots, N_R\}$, the PEP, averaged over channel realizations, can be approximately upper bounded for large SNR values as

$$\mathbb{P}\left(C_{A,k}^{(m)} \to C_{A,k}^{\prime(m)} \right) \stackrel{<}{\sim} \frac{\left(\frac{16 N_R \log \Omega}{\Omega T} \right)^{N_R}}{\Delta \left(C_{A,k}^{(m)}, C_{A,k}^{\prime(m)} \right)} \qquad (20)$$

where $\Omega = \sqrt{\frac{2}{T} \frac{(P_A + P_B + \sigma^2) \sum_{r=1}^{N_R} P_r}{\sigma^2}}$, and $\Delta(C, C') = \det \left((C - C')^* (C - C') \right)$ gives an indication of the distance

between C and C'. With the assumption that $\frac{\sum_{r=1}^{N_R} P_r}{\sigma^2} \gg 1$, the JBD-DSTC scheme can achieve a diversity of $N_R \left(1 - \frac{\log\log \Omega}{\log \Omega}\right)$.

5. NUMERICAL RESULTS

As an example, we consider a frequency-selective Rayleigh fading channel with three taps defined by $\{\sigma_{ir,l}\}_{l \in \{1,2,3\}} = \frac{[1, 0.8, 0.6]}{\sqrt{2}}$, $i \in \{A, B\}$, $r \in \{1, 2, \ldots, N_R\}$, $N = 64$ subcarriers and total bandwidth of 8 kHz. The selection of the available bandwidth is consistent with, for example, underwater acoustic communications. The SNR at user i while detecting the signal of user i' is defined as $SNR_i = (G_1 + G_2) P_{i'}/\sigma_{i,eff}^2$, $i, i' \in \{A, B\}$, $i' \neq i$ where $\sigma_{i,eff}^2 = G_1\sigma_1^2 + G_2\sigma_2^2 + \sigma_i^2$ is the effective noise variance at user i. Unless stated otherwise, Quadrature PSK is used and $\sigma_B^2 = \sigma_1^2 = \sigma_2^2 = \sigma^2$. We further assume that $N_R = 2$, $P_A = 1$, $G_1 = G_2 = 1$, $d_{A1} = 5$, $d_{B1} = 14$, $d_{A2} = 3$, $d_{B2} = 9$, $d_{1B} = 14$ and $d_{2B} = 9$. For the JBD-DSTC scheme, two blocks per group ($T = 2$) is assumed, and we adopt the dispersion matrices designed in [20].

In Figure 3, we compare the BER performance of the JBD detector with that of the coherent detector. Clearly, the coherent scheme outperforms the differential scheme by almost 3 dB which is an expected result. We also plot the performance of a genie-aided differential detector that assumes the knowledge of $\mu_{1,k}$ and $\mu_{2,k}$ $\forall k$, at user B and the knowledge of $\nu_{1,k}$ and $\nu_{2,k}$ $\forall k$, at user A, and hence self-interference is perfectly removed. As seen in Figure 3, if 15 blocks are assumed, the performances of the two schemes match closely, which shows the accuracy of the parameters estimation. Furthermore, it shows that our proposed JBD scheme still performs close to the genie-aided case even if the number of blocks is reduced from 15 to 10.

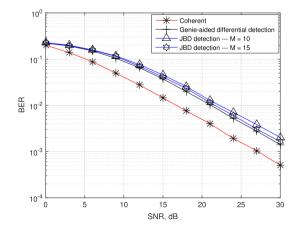Figure 4 compares the JBD-DSTC detector with $M_G = 150$ to the detectors performing coherent DSTC and
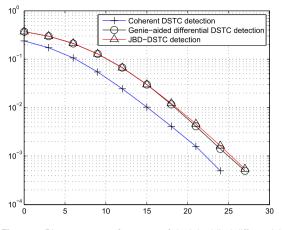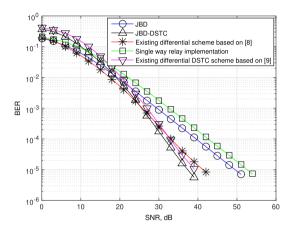

Figure 4. Bit error rate performance of the joint blind-differential (JBD)- distributed space–time coding (DSTC) detector and the coherent DSTC detector.

Figure 5. Bit error rate (BER) performance of the proposed schemes and some existing schemes ($M = 200$). DSTC, distributed space–time coding; JBD, joint blind-differential; SNR, signal-to-noise ratio.

Figure 3. Bit error rate (BER) performance of the joint blind-differential (JBD) detector and the coherent detector. SNR, signal-to-noise ratio.

genie-aided differential DSTC. The latter assumes that the channels corresponding to the self-interference are known for each user, and hence the self-interference is perfectly removed. The results show the accuracy of the proposed scheme as it approaches the performance of the genie-aided system. Also, similar to the JBD scheme, the JBD-DSTC scheme has around a 3 dB loss compared with coherent DSTC.

In Figure 5, we compare our proposed schemes with two existing differential-based TWR schemes along with the conventional single-way relay (SWR) implementation when the channel is quasi-static. For SWR implementation, four phases of transmission are required, and hence we use Quadrature PSK rather than BPSK as in the TWR schemes to unify the transmission rate. For the two schemes in [8,9], we properly extend their proposals to the multicarrier case to perform the comparison. Clearly, the JBD scheme outperforms the JBD-DSTC scheme for SNR values below

17 dB for this example, while the opposite happens for higher SNR values as JBD-DSTC approaches the full diversity order of 2. In fact, the JBD-DSTC scheme outperforms all the other considered schemes for SNR values above 25 dB. Specifically, it outperforms the scheme in [9], the one in [8], the JBD scheme and the SWR system by about 1.5 dB, 1.7 dB, 8.2 dB, and 11.3 dB, respectively, at a BER of about 10^{-4}. Specifically, we attribute the improvement over the scheme in [9], which is also based on differential DSTC, to the fact that the detector in [9] uses estimates of the partner's previous symbol (in addition to the currently received signal) to detect the partner's current symbol, which causes error propagation. In our scheme, on the other hand, the detection of the current symbol is independent from the previous symbol.

We can note from Figure 5 that the scheme in [8] which is based on relay selection diversity performs better than all other proposals for SNR values below 25 dB for this example. However, it imposes a transmission overhead as it requires sending a sufficient number of pilot symbols to aid in assigning specific subcarrier(s) to each relay, and after that, additional feedback is required to broadcast the indices of the subcarriers that each relay should handle. Furthermore, unlike our schemes which only requires simple operations such as complex conjugation and time-reversal at the relays, the scheme in [8] require the relays to perform DFT and IDFT to enable filtering out all subcarriers except the ones assigned to each one of them.

To quantify this difference, let us compare the time complexity of the (major) operations required at the relay for the two schemes. For the proposed schemes, the time reversal operation corresponds to swapping elements of an array from one end to the other, hence this algorithm has time complexity $\mathcal{O}(N)$, and as conjugation is performed in a symbol-wise manner, it has a time complexity $\mathcal{O}(N)$. Therefore, the relay processing of the proposed schemes has time complexity $\mathcal{O}(2N)$. On the other hand, for the scheme in [8], assuming that the DFT is efficiently computed using the fast Fourier transform algorithm which has a complexity of $\mathcal{O}(N \log_2 N)$, then the relay processing (DFT and IDFT) has time complexity $\mathcal{O}(2N \log_2 N)$. This clearly shows the that the complexity of the proposed schemes is much less than that of the scheme in [8] for practical values of N.

Figure 6 compares the analytical and the simulation performance results for the JBD scheme with BPSK modulation using various number of relays. Herein, the power at the relay is normalized as explained in Section 3.3 and the transmit power of the rth relay, P_r, $r \in \{1, 2, \ldots, N_R\}$ is set to unity. Figure 6 shows a close match between simulation results and the analytical P_b (as in (15)) for SNR values greater than 15 dB.

In Figure 7, we compare between the analytical PEP upper bound of the JBD-DSTC detector in (20) with the estimated PEP obtained from Monte Carlo simulations. We consider two scenarios for the number of relays, namely 2 and 4 which are implemented using groups of sizes
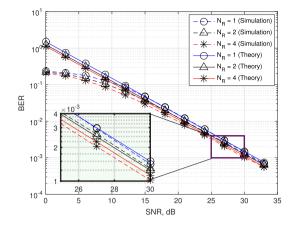

Figure 6. Comparison between analytical and simulation performance results for the joint blind-differential detector ($M = 200$). BER, bit error rate; SNR, signal-to-noise ratio.
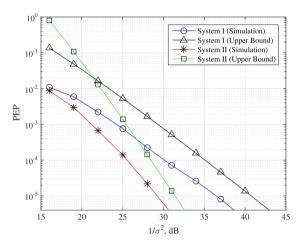

Figure 7. Comparison between analytical PEP upper bound and simulation results for the joint blind-differential-distributed space–time coding detector ($M = 400$).

$T = 2$ and $T = 4$, respectively. Here, we use BPSK modulation, and hence we can adopt the square real orthogonal dispersion matrices proposed in [21]. The following summarizes the structure of the data matrices and the dispersion matrices:

System I

$$C_{i,k}^{(m)} = \frac{1}{\sqrt{\left| X_{i,k}^{(m,1)} \right|^2 + \left| X_{i,k}^{(m,2)} \right|^2}} \begin{bmatrix} X_{i,k}^{(m,1)} & -X_{i,k}^{(m,2)} \\ X_{i,k}^{(m,2)} & X_{i,k}^{(m,1)} \end{bmatrix},$$

$$\tag{21}$$

$$A_1 = I_2 \text{ and } A_2 = \begin{bmatrix} 0 & -1 \\ 1 & 0 \end{bmatrix}. \tag{22}$$

System II

$$C_{i,k}^{(m)} = \frac{1}{\sqrt{\sum_{j=1}^{4}\left|X_{i,k}^{(m,j)}\right|^2}} \begin{bmatrix} X_{i,k}^{(m,1)} & -X_{i,k}^{(m,2)} & -X_{i,k}^{(m,3)} & -X_{i,k}^{(m,4)} \\ X_{i,k}^{(m,2)} & X_{i,k}^{(m,1)} & X_{i,k}^{(m,4)} & -X_{i,k}^{(m,3)} \\ X_{i,k}^{(m,3)} & -X_{i,k}^{(m,4)} & X_{i,k}^{(m,1)} & X_{i,k}^{(m,2)} \\ X_{i,k}^{(m,4)} & X_{i,k}^{(m,3)} & -X_{i,k}^{(m,2)} & X_{i,k}^{(m,1)} \end{bmatrix}, \tag{23}$$

$$A_1 = I_4, \; A_2 = \begin{bmatrix} 0 & -1 & 0 & 0 \\ 1 & 0 & 0 & 0 \\ 0 & 0 & 0 & -1 \\ 0 & 0 & 1 & 0 \end{bmatrix}, \; A_3 = \begin{bmatrix} 0 & 0 & -1 & 0 \\ 0 & 0 & 0 & 1 \\ 1 & 0 & 0 & 0 \\ 0 & -1 & 0 & 0 \end{bmatrix} \text{ and } A_4 = \begin{bmatrix} 0 & 0 & 0 & -1 \\ 0 & 0 & -1 & 0 \\ 0 & 1 & 0 & 0 \\ 1 & 0 & 0 & 0 \end{bmatrix}. \tag{24}$$

Note that for the two systems, $B_r = 0_{T \times T}$, $r \in \{1, 2, \ldots, N_R\}$.

Let $X_{i,k}^{(m)} = \left[X_{i,k}^{(m,1)}, X_{i,k}^{(m,2)}, \ldots, X_{i,k}^{(m,T)}\right]^T$ denote data samples corresponding to the data matrix $C_{i,k}^{(m)}$. Similarly, $X'_{i,k}^{(m)}$ corresponds to $C'_{i,k}^{(m)}$. to maintain fairness between the two scenarios, we consider $X_{i,k}^{(m)} = [1, 1]^T$ and $X'_{i,k}^{(m)} = [-1, -1]^T$ for System I, while for System II, $X_{i,k}^{(m)} = [1, 1, 1, 1]^T$ and $X'_{i,k}^{(m)} = [-1, -1, 1, 1]^T$. Note that for the two scenarios, $\Delta\left(C_{A,k}^{(m)}, C'_{A,k}^{(m)}\right) = 16$. For Figure 7, we assume $P_A = 1$, $P_r = \frac{1}{N_R}$ and $G_r = \left(P_A + P_B + \sigma_r^2\right)^{-1}$, $r \in \{1, 2, \ldots, N_R\}$. Figure 7 shows the validity of the upper bound, and it also shows that the diversity is about 2 and 4 for systems I and II, respectively, as the

PEP drops about 2 and 4 orders of magnitude, respectively, for an SNR increase of 10 dB.

6. CONCLUSIONS

This paper has proposed two schemes for differential asynchronous MR-TWR systems in frequency-selective fading channels in which neither the CSI nor the knowledge of the propagation delays is required. An advantage of these schemes is that the relays are only required to perform simple operations on the received (overlapped) signals,

for example, complex conjugation and time-reversal. Also, after estimating the channel-dependent parameters, only a simple symbol-wise detection rule is required. Through simulations, it is observed that the proposed schemes are superior to the existing ones in the literature. The paper has also provides analytical error probability results for the proposed schemes that match the results of Monte Carlo simulations.

APPENDIX A: SIMPLIFICATION OF $Y_{B,K}^{(M)}$ FOR THE JOINT BLIND-DIFFERENTIAL SCHEME

After DFT, the mth block of the effective signal in frequency-domain can be written as

$$
\begin{aligned}
Y_B^{(m)} &\stackrel{(a)}{=} \sum_{i \in \{A,B\}} \sum_{r=1}^{N_R} \sqrt{P_{ir}} F H_{tl,rB} F^H F \Psi_{d_{rB}} F^H F \eta \left(H_{tl,ir}^* \Psi_{d_{ir}}^* s_i^{(m)*}\right) + F v_B^{(m)} \\
&\stackrel{(b)}{=} \sum_{i \in \{A,B\}} \sum_{r=1}^{N_R} \sqrt{P_{ir}} F H_{tl,rB} F^H F \Psi_{d_{rB}} F^H \left(F H_{tl,ir} \Psi_{d_{ir}} s_i^{(m)}\right)^* + V_B^{(m)} \\
&= \sum_{i \in \{A,B\}} \sum_{r=1}^{N_R} \sqrt{P_{ir}} F H_{tl,rB} F^H F \Psi_{d_{rB}} F^H \left(F H_{tl,ir} F^H F \Psi_{d_{ir}} F^H F s_i^{(m)}\right)^* + V_B^{(m)} \\
&= \sum_{i \in \{A,B\}} \sum_{r=1}^{N_R} \sqrt{P_{ir}} H_{df,rB}^{(m)} \Psi_{F,d_{rB}} \left(H_{df,ir}^{(m)} \Psi_{F,d_{ir}} S_i^{(m)}\right)^* + V_B^{(m)}
\end{aligned}
\tag{A.1}
$$

where $V_B^{(m)} = F v_B^{(m)}$, $\Psi_{F,d} = F \Psi_d F^H$ and (a) follows from the fact that the DFT matrix is a unitary matrix, that is, $F^H F = F F^H = I_N$ where I_N is the size-N identity matrix. The equality (b) follows from the fact that conjugation along with reversal in time-domain results in conjugation in frequency-domain, that is, $F \eta (x^*) = (Fx)^*$.

In case of block or quasi-static fading, which is our assumption here, $H_{tl,ir}$ have a circulant structure causing $H_{df,ir}$ to be diagonal which means no inter-carrier interference is present. When the channel is time-varying within the same OFDM block, neither $H_{tl,ir}$ will be

circulant nor will $H_{df,ir}$ be diagonal, which means that the subcarrier orthogonality is lost, giving rise to inter-carrier interference. It is clear to see that because of the different time delays experienced by the components of the signal in (3.2), different circular shifts resulted. As having a delay of n samples in the time domain causes the kth subcarrier to have a phase shift of $e^{-j2\pi n(k-1)/N}$, $k \in \{1, 2, \ldots, N\}$, we can write the received signal on the kth subcarrier as

$$
y_B^{(m,1)} = \sqrt{P_{A1}} H_{tl,1B} \Psi_{d_{1B}} H_{tl,A1} \Psi_{d_{A1}} s_A^{(m,1)} - \sqrt{P_{A2}} H_{tl,2B} \Psi_{d_{2B}} \eta \left(H_{tl,A2}^* \Psi_{d_{A2}}^* s_A^{(m,2)*} \right)
$$
$$
+ \sqrt{P_{B1}} H_{tl,1B} \Psi_{d_{1B}} H_{tl,B1} \Psi_{d_{B1}} s_B^{(m,1)} - \sqrt{P_{B2}} H_{tl,2B} \Psi_{d_{2B}} \eta \left(H_{tl,B2}^* \Psi_{d_{B2}}^* s_B^{(m,2)*} \right) + v_B^{(m,1)},
$$

(B.3)

$$
y_B^{(m,2)} = \sqrt{P_{A1}} H_{tl,1B} \Psi_{d_{1B}} H_{tl,A1} \Psi_{d_{A1}} s_A^{(m,2)} + \sqrt{P_{A2}} H_{tl,2B} \Psi_{d_{2B}} \eta \left(H_{tl,A2}^* \Psi_{d_{A2}}^* s_A^{(m,1)*} \right)
$$
$$
+ \sqrt{P_{B1}} H_{tl,1B} \Psi_{d_{1B}} H_{tl,B1} \Psi_{d_{B1}} s_B^{(m,2)} + \sqrt{P_{B2}} H_{tl,2B} \Psi_{d_{2B}} \eta \left(H_{tl,B2}^* \Psi_{d_{B2}}^* s_B^{(m,1)*} \right) + v_B^{(m,2)},
$$

(B.4)

$$
Y_{B,k}^{(m)} = \sum_{i \in \{A,B\}} \sum_{r=1}^{N_R} \sqrt{P_{ir}} \left[H_{df,rB}^{(m)} \right]_{k,k}
$$
$$
\times \left[H_{df,ir}^{(m)} \right]_{k,k}^* e^{-j\frac{2\pi(k-1)(d_{rB}-d_{ir})}{N}} S_{i,k}^{(m)*} + V_{B,k}^{(m)},
$$

As we assumed the channels to be reciprocal, then for all $i \in \{A, B\}$, $r \in \{1, 2\}$, $H_{df,ir} = H_{df,ri}$. We also assume that $d_{ri} = d_{ir}$, $r \in \{1, 2\}$, $i \in \{A, B\}$. Therefore, the received signal on the kth subcarrier during the mth block can be written as $Y_{B,k}^{(m)} = \mu_k S_{B,k}^{(m)*} + \nu_k S_{A,k}^{(m)*} + V_{B,k}^{(m)}$.

APPENDIX B: ILLUSTRATIVE EXAMPLE FOR THE JOINT BLIND-DIFFERENTIAL-DISTRIBUTED SPACE–TIME CODING SCHEME: DUAL-RELAY CASE

To clearly illustrate the resulting DSTC structure, we consider the case of having two relays ($N_R = 2$) and using two blocks per group ($T = 2$). For this case, we adopt the dispersion matrices design in [20] that results in Alamouti's code structure. Specifically, the relays' matrices are chosen as

$$
A_1 = \begin{bmatrix} 1 & 0 \\ 0 & 1 \end{bmatrix}, \ B_1 = 0_{T \times T},
$$
$$
A_2 = 0_{T \times T} \text{ and } B_2 = \begin{bmatrix} 0 & -1 \\ 1 & 0 \end{bmatrix}.
$$

(B.1)

Interestingly, for the case of $N_R = 2$ and $T = 2$, it was found in [20] that a space–time codeword, C, satisfies the commutative property if and only if it follows the 2×2 Alamouti structure. Hence, $C_{i,k}^{(m)}$ is constructed as

$$
C_{i,k}^{(m)} = \frac{1}{\sqrt{\left| X_{i,k}^{(m,1)} \right|^2 + \left| X_{i,k}^{(m,2)} \right|^2}} \begin{bmatrix} X_{i,k}^{(m,1)} & -X_{i,k}^{(m,2)*} \\ X_{i,k}^{(m,2)} & X_{i,k}^{(m,1)*} \end{bmatrix}.
$$

(B.2)

After removing the CP of length $N_{CP,2}$ at user B, the resulting two consecutive N-sample OFDM blocks of the mth group, $m \in \{1, M_G\}$, can be written as

where $v_B^{(m,t)}$ represents length-N effective noise vector at user B during the tth block of the mth group whose entries are AWGN random variables with zero mean and variance of σ_B^2.

After performing DFT, the frequency-domain signal corresponding to the first block of the mth group can be written as

$$
Y_B^{(m,1)} =
$$
$$
\sqrt{P_{A1}} F H_{tl,1B} F^H F \Psi_{d_{1B}} F^H F H_{tl,A1} F^H F \Psi_{d_{A1}} s_A^{(m,1)}
$$
$$
- \sqrt{P_{A2}} F H_{tl,2B} F^H F \Psi_{d_{2B}} F^H F \eta \left(H_{tl,A2}^* \Psi_{d_{A2}}^* s_A^{(m,2)*} \right)
$$
$$
+ \sqrt{P_{B1}} F H_{tl,1B} F^H F \Psi_{d_{1B}} F^H F H_{tl,B1} F^H F \Psi_{d_{B1}} F^H F s_B^{(m,1)}
$$
$$
- \sqrt{P_{B2}} F H_{tl,2B} F^H F \Psi_{d_{2B}} F^H F \eta
$$
$$
\times \left(H_{tl,B2}^* \Psi_{d_{B2}}^* s_B^{(m,2)*} \right) + V_B^{(m,1)}
$$
$$
= \sqrt{P_{A1}} H_{df,1B} \Psi_{F,d_{1B}} H_{df,A1} \Psi_{F,d_{A1}} S_A^{(m,1)}
$$
$$
- \sqrt{P_{A2}} H_{df,2B} \Psi_{F,d_{2B}} \left(H_{df,A2} \Psi_{F,d_{A2}} S_A^{(m,2)} \right)^*
$$
$$
+ \sqrt{P_{B1}} H_{df,1B} \Psi_{F,d_{1B}} H_{df,B1} \Psi_{F,d_{B1}} S_B^{(m,1)}
$$
$$
- \sqrt{P_{B2}} H_{df,2B} \Psi_{F,d_{2B}} \left(H_{df,B2} \Psi_{F,d_{B2}} S_B^{(m,2)} \right)^*
$$
$$
+ V_B^{(m,1)}
$$

(B.5)

where $V_B^{(m,t)} = F v_B^{(m,t)}$. Similarly, we can write $Y_B^{(m,2)}$ for the second block as

$$
Y_B^{(m,2)} = \sqrt{P_{A1}} H_{df,1B} \Psi_{F,d_{1B}} H_{df,A1} \Psi_{F,d_{A1}} S_A^{(m,2)}
$$
$$
+ \sqrt{P_{A2}} H_{df,2B} \Psi_{F,d_{2B}} \left(H_{df,A2} \Psi_{F,d_{A2}} S_A^{(m,1)} \right)^*
$$
$$
+ \sqrt{P_{B1}} H_{df,1B} \Psi_{F,d_{1B}} H_{df,B1} \Psi_{F,d_{B1}} S_B^{(m,2)}
$$
$$
+ \sqrt{P_{B2}} H_{df,2B} \Psi_{F,d_{2B}} \left(H_{df,B2} \Psi_{F,d_{B2}} S_B^{(m,1)} \right)^*
$$
$$
+ V_B^{(m,2)}.
$$

(B.6)

With $Y_{B,k}^{(m)} = \left[Y_{B,k}^{(m,1)}, Y_{B,k}^{(m,2)} \right]^T$ and $V_{B,k}^{(m)} = \left[V_{B,k}^{(m,1)}, V_{B,k}^{(m,2)} \right]^T$, we can write $Y_{B,k}^{(m)}$ as

$$Y_{B,k}^{(m)} = D_{B,k}^{(m)} \mu_{B,k} + D_{A,k}^{(m)} \mu_{A,k} + V_{B,k}^{(m)}, \qquad (B.7)$$

where

$$D_{i,k}^{(m)} = \begin{bmatrix} S_{i,k}^{(m,1)} & -S_{i,k}^{(m,2)*} \\ S_{i,k}^{(m,2)} & S_{i,k}^{(m,1)*} \end{bmatrix}, \quad i \in \{A, B\}, \qquad (B.8)$$

$$\mu_{B,k}^{(m)} = \begin{bmatrix} \sqrt{P_{B1}} \left[H_{df,1B}^{(m)} \right]_{k,k} \left[H_{df,B1}^{(m)} \right]_{k,k} e^{-j\frac{2\pi(k-1)\left(d_{1B}+d_{B1}\right)}{N}} \\ \sqrt{P_{B2}} \left[H_{df,2B}^{(m)} \right]_{k,k} \left[H_{df,B2}^{(m)} \right]_{k,k}^* e^{-j\frac{2\pi(k-1)\left(d_{2B}-d_{B2}\right)}{N}} \end{bmatrix}, \qquad (B.9)$$

and

$$\mu_{A,k}^{(m)} = \begin{bmatrix} \sqrt{P_{A1}} \left[H_{df,1B}^{(m)} \right]_{k,k} \left[H_{df,A1}^{(m)} \right]_{k,k} e^{-j\frac{2\pi(k-1)\left(d_{1B}+d_{A1}\right)}{N}} \\ \sqrt{P_{A2}} \left[H_{df,2B}^{(m)} \right]_{k,k} \left[H_{df,A2}^{(m)} \right]_{k,k}^* e^{-j\frac{2\pi(k-1)\left(d_{2B}-d_{A2}\right)}{N}} \end{bmatrix}. \qquad (B.10)$$

APPENDIX C: ESTIMATION OF THE SELF-INTERFERENCE TERM IN THE JBD-DSTC SCHEME

As a first step we investigate the expected value of $D_{B,k}^{(m)H} Y_{B,k}^{(m)}$ over the constellation points of $S_{A,k}^{(m)}$ and $S_{B,k}^{(m)}$. We can write this as $\mathbb{E}\left[D_{B,k}^{(m)H} Y_{B,k}^{(m)} \right] = \mathbb{E}\left[D_{B,k}^{(m)H} D_{B,k}^{(m)} \right] \mu_{B,k} + \mathbb{E}\left[D_{B,k}^{(m)H} D_{A,k}^{(m)} \right] \mu_{A,k} + V_{B,k}^{(m)}$.

To simplify exposition, and because we aim to take the expectation over the constellation points rather than time or frequency, we will drop the subcarrier index (k) and the block index (m) such that $D_{i,k}^{(m)}$, $\widetilde{S}_{i,k,r}^{(m)}$ and $\widetilde{S}_{i,k,r}^{(m,t)}$ will be expressed by D_i, $\widetilde{S}_{i,r}$ and $\widetilde{S}_{i,r}^{(t)}$, respectively. We can write $D_B^H D_B$ as

where we used the fact $O_r^H O_r = I_T$. Let $J^{i,j} = O_i^H O_j$ and let its element in the (l, p) position be denoted by $J_{l,p}^{i,j}$. Recall that $J^{i,j}$, $i \neq j$, is a hollow matrix, that is, $J_{l,l}^{i,j} = 0$ $\forall l \in \{1, 2, \ldots, T\}$.

Note that $\widetilde{S}_{B,i}^H J^{i,j} \widetilde{S}_{B,j} = \sum_{r=1}^{T} \widetilde{S}_{B,i}^{(r)*} \sum_{c=1}^{T} J_{r,c}^{i,j} \widetilde{S}_{B,j}^{(c)} = \sum_{r=1}^{T} \sum_{c=1}^{T} J_{r,c}^{i,j} \widetilde{S}_{B,i}^{(r)*} \widetilde{S}_{B,j}^{(c)}$. Hence, we can write $\mathbb{E}\left[\widetilde{S}_{B,i}^H J^{i,j} \widetilde{S}_{B,j} \right] = \sum_{r=1}^{T} \sum_{c=1}^{T} J_{r,c}^{i,j} \mathbb{E}\left[\widetilde{S}_{B,i}^{(r)*} \widetilde{S}_{B,j}^{(c)} \right]$. Due to the differential encoding, both $\widetilde{S}_{B,i}^{(r)}$ and $\widetilde{S}_{B,j}^{(c)}$ are correlated because they both consist of differently-weighted linear combination of the same T random variables, which on the other hand, are also correlated with each other because of the same reason. However, by examining their correlation coefficients, we have found that they are small enough to be neglected. Therefore, we approximate their correlation by zero, and hence $\mathbb{E}\left[\widetilde{S}_{B,i}^H J^{i,j} \widetilde{S}_{B,j} \right] \approx 0$, $i \neq j$, and $\mathbb{E}\left[D_B^H D_B \right] \approx T I_{N_R}$. Following the same rationale, we conclude that $\mathbb{E}\left[D_B^H D_A \right] \approx 0_{N_R \times N_R}$.

Finally, assuming large M, we use the law of large numbers to approximate the expected value of $D_{B,k}^{(m)H} Y_{B,k}^{(m)}$ by its time average, which can be calculated at user B, as $\sum_{m=1}^{M} D_{B,k}^{(m)H} Y_{B,k}^{(m)} / M$, and hence we obtain $\widehat{\mu}_{B,k} \approx \sum_{m=1}^{M} D_{B,k}^{(m)H} Y_{B,k}^{(m)} / (MT)$ for large SNRs.

ACKNOWLEDGEMENTS

REFERENCES

1. Salim A, Duman TM. An asynchronous two-way relay system with full delay diversity in time-varying multipath environments. In *IEEE International Conference on Computing, Networking and Communications (ICNC)*, Feb. 2015; 900–904.

$$D_B^H D_B = \begin{bmatrix} \widetilde{S}_{B,1}^H O_1^H O_1 \widetilde{S}_{B,1} & \widetilde{S}_{B,1}^H O_1^H O_2 \widetilde{S}_{B,2} & \cdots & \widetilde{S}_{B,1}^H O_1^H O_{N_R} \widetilde{S}_{B,N_R} \\ \widetilde{S}_{B,2}^H O_2^H O_1 \widetilde{S}_{B,1} & \widetilde{S}_{B,2}^H O_2^H O_2 \widetilde{S}_{B,2} & \cdots & \widetilde{S}_{B,2}^H O_2^H O_{N_R} \widetilde{S}_{B,N_R} \\ \vdots & \vdots & \ddots & \vdots \\ \widetilde{S}_{B,N_R}^H O_{N_R}^H O_1 \widetilde{S}_{B,1} & \cdots & \cdots & \widetilde{S}_{B,N_R}^H O_{N_R}^H O_{N_R} \widetilde{S}_{B,N_R} \end{bmatrix}, \qquad (C.1)$$

$$= \begin{bmatrix} T & \widetilde{S}_{B,1}^H O_1^H O_2 \widetilde{S}_{B,2} & \cdots & \widetilde{S}_{B,1}^H O_1^H O_{N_R} \widetilde{S}_{B,N_R} \\ \widetilde{S}_{B,2}^H O_2^H O_1 \widetilde{S}_{B,1} & T & \cdots & \widetilde{S}_{B,2}^H O_2^H O_{N_R} \widetilde{S}_{B,N_R} \\ \vdots & \vdots & \ddots & \vdots \\ \widetilde{S}_{B,N_R}^H O_{N_R}^H O_1 \widetilde{S}_{B,1} & \cdots & \cdots & T \end{bmatrix}, \qquad (C.2)$$

2. Salim A, Duman TM. A delay-tolerant asynchronous two-way-relay system over doubly-selective fading channels. *IEEE Transactions on Wireless Communications* 2015; **14**(7): 3850–3865.

3. Song L, Li Y, Huang A, Jiao B, Vasilakos A. Differential modulation for bidirectional relaying with analog network coding. *IEEE Transactions on Signal Processing* 2010; **58**(7): 3933–3938.

4. Cui T, Gao F, Tellambura C. Differential modulation for two-way wireless communications: a perspective of differential network coding at the physical layer. *IEEE Transactions on Communications* 2009; **57**(10): 2977–2987.

5. Guan W, Liu K. Performance analysis of two-way relaying with non-coherent differential modulation. *IEEE Transactions on Wireless Communications* 2011; **10**(6): 2004–2014.

6. Zhu K, Burr A. A simple non-coherent physical-layer network coding for transmissions over two-way relay channels. In *IEEE Global Communications Conference (GLOBECOM)*, Anaheim, California, 2012; 2268–2273.

7. Bhatnagar MR. Making two-way satellite relaying feasible: a differential modulation based approach. *IEEE Transactions on Communications* 2015; **63**(8): 2836–2847.

8. Song L, Hong G, Jiao B, Debbah M. Joint relay selection and analog network coding using differential modulation in two-way relay channels. *IEEE Transactions on Vehicular Technology* 2010; **59**(6): 2932–2939.

9. Utkovski Z, Yammine G, Lindner J. A distributed differential space-time coding scheme for two-way wireless relay networks. In *IEEE International Symposium on Information Theory*, Seoul, Korea, 2009; 779–783.

10. Huo Q, Song L, Li Y, Jiao B. A distributed differential space-time coding scheme with analog network coding in two-way relay networks. *IEEE Transactions on Signal Processing* 2012; **60**(9): 4998–5004.

11. Alabed S, Pesavento M, Klein A. Distributed differential space-time coding for two-way relay networks using analog network coding. In *the 21st European Signal Processing Conference (EUSIPCO)*, Marrakech, Morocco, 2013; 1–5.

12. Wu Z, Liu L, Jin Y, Song L. Signal detection for differential bidirectional relaying with analog network coding under imperfect synchronisation. *IEEE Communications Letters* 2013; **17**(6): 1132–1135.

13. Qian M, Jin Y, Wu Z, Wang T. Asynchronous two-way relaying networks using distributed differential space-time coding. *International Journal of Antennas and Propagation* 2015; **2015**: 9 pages, Article ID 563737.

14. Avendi MR, Jafarkhani H. Differential distributed space–time coding with imperfect synchronization in frequency-selective channels. *IEEE Transactions on Wireless Communications* 2015; **14**(4): 1811–1822.

15. Fang Z, Zheng L, Wang L, Jin L. A frequency domain differential modulation scheme for asynchronous amplify-and-forward relay networks. In *IEEE China Summit and International Conference on Signal and Information Processing (ChinaSIP)*, Chengdu, China, July 2015; 977–981.

16. Wei R-Y. Differential encoding for quadrature-amplitude modulation. In *IEEE Vehicular Technology Conference (VTC)*, Ottawa, Canada, May 2010; 1–5.

17. Divsalar D, Simon MK. Multiple-symbol differential detection of mpsk. *IEEE Transactions on Communications* 1990; **38**(3): 300–308.

18. Hasna M, Alouini M-S. End-to-end performance of transmission systems with relays over Rayleigh-fading channels. *IEEE Transactions on Wireless Communications* 2003; **2**(6): 1126–1131.

19. Jing Y, Hassibi B. Distributed space-time coding in wireless relay networks. *IEEE Transactions on Wireless Communications* 2006; **5**(12): 3524–3536.

20. Jing Y, Jafarkhani H. Distributed differential space-time coding for wireless relay networks. *IEEE Transactions on Communications* 2008; **56**(7): 1092–1100.

21. Tarokh V, Jafarkhani H, Calderbank A. Space-time block codes from orthogonal designs. *IEEE Transactions on Information Theory* 1999; **45**(5): 1456–1467.

AUTHORS' BIOGRAPHIES

Ahmad Salim is a Post-Doctoral Research Associate in the Department of Electrical and Computer Engineering at the University of Illinois at Chicago, Illinois, USA. He received his BS degree in Electrical Engineering from the University of Jordan, Amman, Jordan, in 2006. Later, he received his MS in Telecommunication Engineering from King Fahd University of Petroleum and Minerals, Dhahran, Saudi Arabia, in 2010. In 2015, he received his PhD in Electrical Engineering from Arizona State University, Arizona, USA. Broadly speaking, his research belongs to the areas of communications theory, information theory and signal processing, including wireless communications, underwater acoustic communications, cooperative communications, MIMO systems, diversity techniques, error control coding, and iterative receivers. Dr. Salim achieved the eighth place in Jordan's 2006 nationwide comprehensive examination in the Electrical Engineering discipline. He is an active participant of the Sensor, Signal and Information

Processing (SenSIP) Center of Arizona State University. He served as a reviewer for IEEE Transactions on Wireless Communications, IEEE Wireless Communications Letters, IEEE Transactions on Vehicular Technology, and Elsevier Physical Communication among others. He is a member of the Communication Theory Technical Committee.

Tolga M. Duman is a Professor of Electrical and Electronics Engineering Department of Bilkent University in Turkey, and an adjunct professor with the School of ECEE at Arizona State University. He received the BS degree from Bilkent University in Turkey in 1993, MS and PhD degrees from Northeastern University, Boston, in 1995 and 1998, respectively, all in electrical engineering. Prior to joining Bilkent University in September 2012, he has been with the Electrical Engineering Department of Arizona State University first as an Assistant Professor (1998–2004), as an Associate Professor (2004–2008), and as a Professor (2008–2015). Dr. Duman's current research interests are in systems, with particular focus on communication and signal processing, including wireless and mobile communications, coding/modulation, coding for wireless communications, data storage systems and underwater acoustic communications. Dr. Duman is a Fellow of IEEE, a recipient of the National Science Foundation CAREER Award and IEEE Third Millennium medal. He served as an editor for IEEE Trans. on Wireless Communications (2003–2008), IEEE Trans. on Communications (2007–2012), and IEEE Online Journal of Surveys and Tutorials (2002–2007). He is currently the coding and communication theory area editor for IEEE Trans. on Communications (2011–present) and an editor for Elsevier Physical Communications Journal (2010–present).